Fort Hays State University

FHSU Scholars Repository

1-1-1997

The role of HO$_X$ in super- And subsonic aircraft exhaust plumes

T. F. Hanisco
Harvard University

P. O. Wennberg
Harvard University

R. C. Cohen
Harvard University

J. G. Anderson
Harvard University

D. W. Fahey
National Oceanic and Atmospheric Administration

See next page for additional authors

Recommended Citation

Hanisco, T. F., Wennberg, P. O., Cohen, R. C., Anderson, J. G., Fahey, D. W., Keim, E. R., Gao, R. S., Wamsley, R. C., Donnelly, S. G., Negro, L. A. D., Salawitch, R. J., Kelly, K. K., & Proffitt, M. H. (1997). The role of HOx in super- and subsonic aircraft exhaust plumes. Geophysical Research Letters, 24(1), 65–68. https://doi.org/10.1029/96GL03724

Authors

T. F. Hanisco, P. O. Wennberg, R. C. Cohen, J. G. Anderson, D. W. Fahey, E. R. Keim, R. S. Gao, R. C. Wamsley, Stephen G. Donnelly Ph.D., L. A. Del Negro, R. J. Salawitch, K. K. Kelly, and M. H. Proffitt

The role of HO_x in super- and subsonic aircraft exhaust plumes

T. F. Hanisco,[1] P. O. Wennberg,[1] R. C. Cohen,[1] J. G. Anderson,[1] D. W. Fahey,[2] E. R. Keim,[2] R. S. Gao,[2,3] R. C. Wamsley,[2,3] S. G. Donnelly,[2,3] L. A. Del Negro,[2,3] R. J. Salawitch,[4] K. K. Kelly[2] and M. H. Proffitt.[2,3]

Abstract. The generation of sulfuric acid aerosols in aircraft exhaust has emerged as a critical issue in determining the impact of supersonic aircraft on stratospheric ozone. It has long been held that the first step in the mechanism of aerosol formation is the oxidation of SO_2 emitted from the engine by OH in the exhaust plume. We report in situ measurements of OH and HO_2 in the exhaust plumes of a supersonic (Air France Concorde) and a subsonic (NASA ER-2) aircraft in the lower stratosphere. These measurements imply that reactions with OH are responsible for oxidizing only a small fraction of SO_2 (2%), and thus cannot explain the large number of particles observed in the exhaust wake of the Concorde.
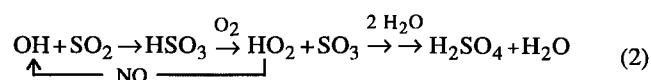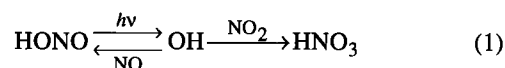
Introduction

Emissions from a proposed fleet of commercial high speed civil transports (HSCT's) flying in the lower stratosphere may alter stratospheric ozone concentrations. Concerns that reactive nitrogen emissions ($NO_x = NO + NO_2$) could substantially deplete ozone helped deter the development of HSCT's in the U.S. during the early 1970's and continue to influence HSCT engine design today [Stolarski et al., 1995]. In the mid- to upper-stratosphere, direct removal of ozone by NO_x is thought to account for most of the catalytic destruction of ozone; thus increased NO_x could increase ozone loss rates. However, in the lower stratosphere, NO_x suppresses the concentrations of HO_2 and ClO that together can dominate the ozone loss rate [Wennberg et al., 1994a]. Thus, in the lower stratosphere, increased NO_x can lead to decreased ozone loss rates. The current assessment of the potential effects of HSCT emissions reflects this picture: NO_x emissions are predicted to enhance ozone loss rates in the middle stratosphere and decrease ozone loss rates in the lower stratosphere. This cancellation results in a small net change in the ozone column at most latitudes.

Recent observations of the exhaust emitted from an Air France Concorde during supersonic flight in the lower stratosphere show that the measured NO_x emission index agrees well with predictions based on ground-based tests performed in the early 70's [Fahey et al., 1995a]. However, the number of volatile particles measured, assumed to consist largely of sulfuric acid generated from fuel sulfur, is much higher than expected. Thus, HSCT emissions could significantly increase aerosol surface area in the lower stratosphere. This is a critical

issue because in the lower stratosphere reactions occurring on these aerosols suppress the concentration of NO_x. Ironically, HSCT particle emissions could increase ozone loss rates by reducing the concentration of NO_x in the lower stratosphere.

Though the mechanism for aerosol formation in aircraft exhaust is not known in detail, the initial step in sulfate aerosol formation has long been assumed to be the oxidation of emitted SO_2 by OH in the aircraft exhaust wake [Stolarski et al., 1995]. In the absence of oxidation within the engine, the production rate of nitric and sulfuric acid is controlled by the following reaction sequences occurring in the exhaust plume:

$$HONO \underset{NO}{\overset{h\nu}{\rightleftarrows}} OH \xrightarrow{NO_2} HNO_3 \qquad (1)$$

$$OH + SO_2 \underset{NO}{\overset{O_2}{\rightarrow}} HSO_3 \rightarrow HO_2 + SO_3 \xrightarrow{2 H_2O} \rightarrow \rightarrow H_2SO_4 + H_2O \qquad (2)$$

In this high NO_x environment, the reactions in (1) dominate the photochemistry that controls the concentration of OH. As the exhaust leaves the engine, OH is sequestered into nitrous acid (HONO) which serves as a temporary reservoir for emitted OH [Arnold et al., 1992]. During daylight OH is produced from the photolysis of HONO and is either converted back to HONO by NO or to HNO_3 by NO_2. The oxidation of SO_2 and the subsequent production of H_2SO_4 occurs while HONO is photolyzed: in darkness no oxidation will occur and in the absence of NO_2 the oxidation of SO_2 could occur indefinitely because it is catalytic with respect to HO_x (= OH + HO_2).

Measurements

The measurements presented here were obtained aboard the NASA ER-2 on October 8, 1994 during the Airborne Southern Hemisphere Ozone Experiment/Measurements for Assessing the Effects of Stratospheric Aircraft (ASHOE/MAESA) campaign in Christchurch, New Zealand. The payload included instruments measuring most of the species necessary to empirically test the chemistry of HO_x in the plume: NO, NO_2, NO_y (= NO_x + HONO + HNO_3 + $ClONO_2$ + $2N_2O_5$ ...), H_2O, O_3, OH and HO_2. Measurements of CH_4 and CO show these species do not play a significant role in HO_x plume chemistry.

Figure 1 shows the OH and HO_2 mixing ratios measured during three crossings of the Concorde exhaust plume (a-c) and an encounter with the ER-2 plume (d). As the plume ages, [OH] (the square brackets denote concentrations) falls markedly. In the early encounters [OH] is above ambient because the production of OH from the photolysis of HONO is large. In the later encounters (e.g. Fig. 1c) [OH] decreases because [HONO] is diminished, weakening the photochemical source of OH, while the loss rate of OH due to reaction with NO_2 remains high. The small [HO_2] in the plume results from a change in the partitioning of HO_x: the high [NO] shifts the

[1]Department of Chemistry, Harvard University, Cambridge, MA
[2]NOAA Aeronomy Laboratory, Boulder, CO
[3]Also at Cooperative Institute for Research in Environmental Science, University of Colorado, Boulder, CO
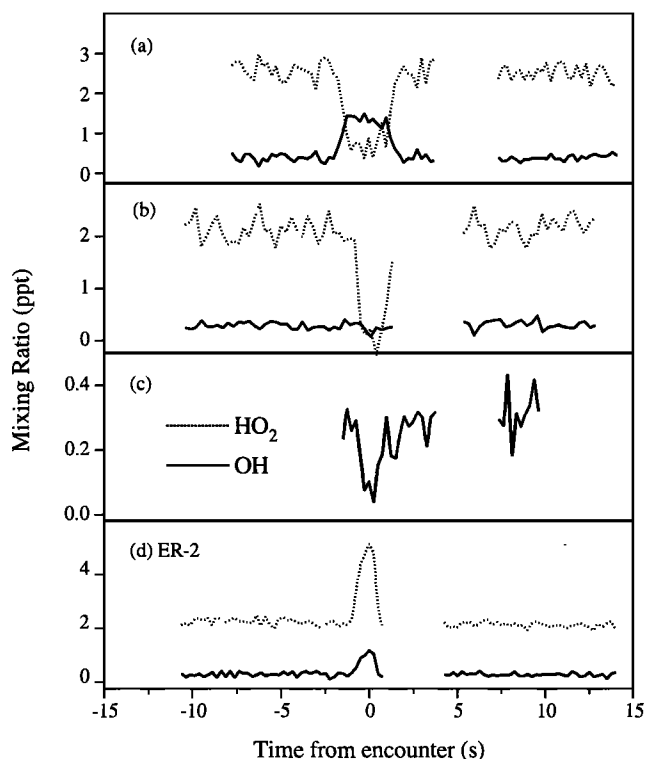[4]Jet Propulsion Laboratory, Pasadena, CA

Figure 1. OH (solid line) and HO$_2$ (broken line) mixing ratios measured during three crossings of the Concorde exhaust plume (a-c) and the single encounter with the ER-2 plume (d). The gaps in the data occur during background calibration of the OH fluorescence signal and (in panel c) during a calibration of the chemical titration of HO$_2$ [*Wennberg et al.*, 1994b]. The plume ages are a) 16, b) 60, and c) 66 minutes for the Concorde exhaust and d) 10 minutes for the ER-2 exhaust. Meteorological conditions are: altitude 16.2 km, temperature 222 K, and pressure 100 mb. The Concorde plumes correspond to encounters 3, 9, and 11 observed by the NO$_y$ instrument [*Fahey et al.*, 1995a].

partitioning of HO$_x$ towards OH because the species that convert OH to HO$_2$ (O$_3$ and CO) do not increase above background levels inside the plume.

The Hydrogen Radical Emission Index

We can infer the [HONO] in the plume by comparing the effective production and loss rates of OH calculated with a steady state photochemical model. The model uses measurements obtained on the ER-2, rate constants from *DeMore et al.*, 1994, and photolysis rates calculated with a radiative transfer model [*Salawitch et al.*, 1994]. Since the lifetime of OH is short (< 1 minute), the steady state solution is representative of conditions in sampled air parcels inside and outside of the plume. The results for encounter #3 (Fig. 1a) are listed in Table 1. Outside the plume the agreement between production and loss rates is excellent. Inside the plume, loss rates increase by two orders of magnitude due to the large increases in [NO] and [NO$_2$], but the increase in production rates due to background species (H$_2$O, HNO$_4$, H$_2$CO) is small. In the absence of added HONO in the plume, the calculated [OH] is a factor of 40 lower than measured.

Since the production rate of OH from HONO photolysis is the only significant undetermined source of OH in the plume, this rate must be equal to the difference between production

and loss rates within the plume (1.48×10^6 molecules/cm^{3}s). The [HONO] inferred from this rate and the photolysis rate of HONO (2.73×10^{-3} s^{-1}) is 5.4×10^8 molecules/cm^3, or 165 ± 65 ppt (1σ). Since the loss rate of OH in the plume is dominated by reactions in (1), the uncertainty of this estimate of HONO is determined by uncertainties in the OH, NO, and NO$_2$ measurements, rate constants, and the photolysis rate of HONO. The contribution of other sources of OH formed in the exhaust are neglected in this estimate, but will be addressed below.

The [HONO] in the plume 981 s prior to this measurement can be estimated using the lifetime of HONO in the plume. Because of the high [NO] and [NO$_2$] in the plume, the lifetime of HONO is determined by the time constant for removal of OH. The net loss rate for HONO in the plume is the fraction of photolyzed HONO that forms HNO$_3$ multiplied by the photolysis rate. The lifetime of HONO in the plume is:

$$\tau = \left[\frac{k_2[OH][NO_2]}{k_1[OH][NO] + k_2[OH][NO_2]} \times J_{HONO} \right]^{-1} \tag{3}$$

For the rates in the plume listed in Table 1, τ = 586 s. Eq. 3 is independent of dilution, so we reference to a conserved tracer, NO$_y$, to account for the effects of dilution and integrate the loss of HONO over the age of the plume. [HONO] referenced to [NO$_y$] at the time of emission (*t* = 0) is:

$$\frac{[HONO]_0}{[NO_y]_0} = \frac{[HONO]_t e^{\frac{t}{\tau}}}{[NO_y]_t}, \tag{4}$$

where the concentrations refer to values above ambient levels. For encounter #3, Eq. 4 yields [HONO]$_0$/[NO$_y$]$_0$ = 0.045, ([NO$_y$]$_t$ = 19 ppb). This [HONO]$_0$ corresponds to the sum of emitted HO$_x$ that forms HONO after emission and any HONO that might be directly emitted from the engine. In the absence of other loss processes for HO$_x$ and HONO the total [HO$_x$]$_0$ emitted from the engine is given by Eq. 4.

An important uncertainty in [HO$_x$]$_0$ calculated from Eq. 4 is the fraction of emitted OH that forms HONO. The small

Table 1. Calculated production and loss rates of OH for encounter #3 (Fig. 1a). Only the most important rates are shown. Rates are in 10^3 molecules/cm^{3}s. Values in parentheses are the percent contribution to the total rate.

	Background Rate		Plume Rate	
		OH Production		
HNO$_3$ + hv	3.5	(26)	4.6	(0)
H$_2$CO + hv	3.5	(26)	9.9	(2)
O (^{1}D) + H$_2$O	2.9	(22)	3.3	(1)
HONO + hv	1.3	(10)	J$_{HONO}$[HONO]	(95)
HNO$_4$ + hv	1.1	(8)	9.6	(2)
total	14.0		1500	
		OH Loss		
OH + HO$_2$	3.2	(21)	5	(0)
OH + NO$_2$	2.9	(19)	852	(57)
OH + HNO$_3$	2.8	(19)	14	(1)
HO$_2$ + NO$_2$	2.2	(14)	39	(3)
OH + NO	1.3	(9)	512	(34)
OH + HNO$_4$	1.2	(8)	32	(2)
total	15.0		1500	

[H$_2$O], [OH], and [NO] are measured. [NO$_2$] is the mean of the measured and calculated steady-state concentrations. [HNO$_3$] is inferred from the NO$_y$ measurement. [H$_2$CO], [HNO$_4$], [O(^{1}D)], and background [HONO] are calculated from steady-state relations. [HONO] in the plume is calculated as described in the text.

[HO$_x$]$_0$/[NO$_x$]$_0$ results in little loss of HO$_x$ through self reactions, but the reaction of OH with NO$_2$ converts some of the emitted OH into HNO$_3$ before HO$_x$ is sequestered into HONO. Ground based tests of the Concorde Olympus engine indicate that NO$_2$ is 4% of emitted NO$_x$ at the engine exit plane [*Williams*, 1973]. Based on the relative rates of OH + NO and OH + NO$_2$, Eq. 4 underestimates [HO$_x$]$_0$ by ~10%. On the other hand, Eq. 4 overestimates [HO$_x$]$_0$ (~6%) by assuming steady state values for NO$_2$/NO for the duration of the plume. These uncertainties, combined with that of the steady-state model result in a net uncertainty of ±50% (1σ) for known processes. If other loss processes for emitted OH occur, the estimate from Eq. 4 will be a lower limit.

The removal of HONO via non-photolytic processes would also result in an underestimation of OH at the exit plane. HONO is known to react in H$_2$SO$_4$/H$_2$O solutions [*Zhang et al.*, 1996; *Fenter and Rossi*, 1996]. Model calculations estimate that up to 25% of HONO could be removed by uptake onto H$_2$SO$_4$/H$_2$O aerosols that might be generated early in the plume (*B. Kärcher*, personal communication, 1996). However, there is substantial uncertainty in this estimate because the surface area and composition of aerosols at the exit plane are not known. It is also not known whether the aerosol reac-
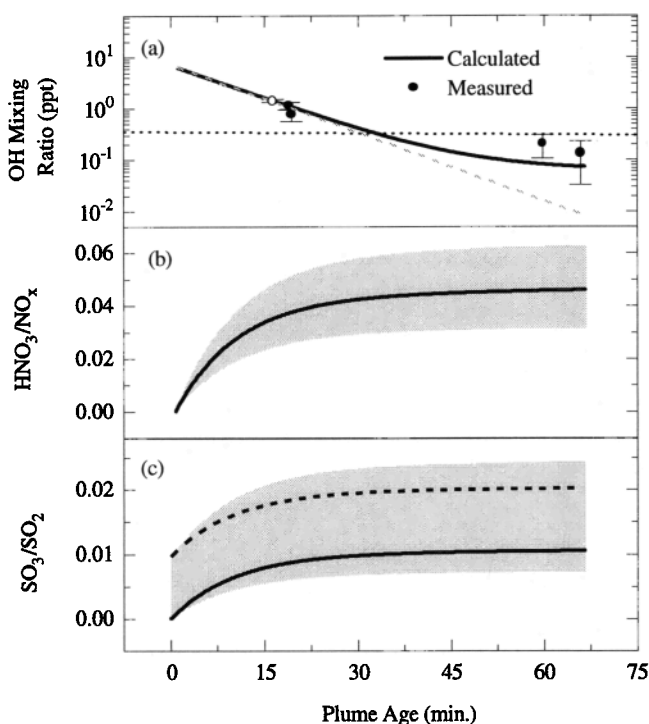

Figure 2. (a) Time evolution of OH produced from HONO photolysis in the Concorde plume. The five measurements (circles) are scaled to [NO$_y$] in each encounter. The error bars are the 2-σ uncertainties of the measurements. The open circle represents encounter #3. The solid line is the result of the integrating model and the dashed line is the result of Eq. 4, each using [HONO]$_0$/[NO$_y$]$_0$ = 0.045. The dotted line corresponds to the 0.3 ppt background level of OH. Oxidation of (b) NO$_2$ → HNO$_3$ and (c) SO$_2$ → SO$_3$ in the plume is shown versus plume age. The oxidation ratio is the ratio of emitted NO$_x$ or SO$_2$ that is oxidized by emitted OH to the total NO$_x$ or SO$_2$ emitted from the engine. The shaded region includes the 1-σ uncertainty of the calculation. The dashed line in (c) represents the oxidation ratio of SO$_2$ assuming all HO$_x$ is emitted as OH, the solid line represents the ratio if OH is converted to HONO prior to emission.

Table 2. Relative HO$_x$ emission indices:

Encounter	$\dfrac{[HO_x]_0}{[NO_y]_0}$	EI NO$_y$ [†] (gNO$_2$/kg fuel)	EI HO$_x$ (gOH/kg fuel)
Concorde #3	0.045	23	0.35 ± 0.17
Concorde #4-5	0.051	<12	0.2 ± 0.1
ER-2	0.035	4	0.06 ± 0.02

[†] NO$_y$ emission indices are from *Fahey, et al.*, 1995a; 1995b.

tivity would saturate due to uptake of HONO (there are *at least* three HONO molecules for every sulfur atom in the fuel). Finally, the measured NO$_x$/NO$_y$ (0.9) is inconsistent with the conversion of large amounts of HO$_x$ into HNO$_3$.

Given the estimate of HONO at the time of emission, the time evolution of OH in the plume can be calculated using an integrating photochemical model. The model solves the coupled differential equations that control OH concentrations (see Table 1) using measured concentrations and temperatures, calculated photolysis rates, and [HONO]$_0$ calculated from Eq. 4. The results using the conditions for encounter #3 as model inputs are compared to the measurements of OH in Figure 2.

The agreement of this model with the measured OH for encounter #3 shows that the assumptions in the calculation of HONO discussed above are justified. In fact, the more extensive photochemical model and Eq. 4 give nearly identical results until the plume is more than 15 min. old. This agreement occurs because HONO is the primary source of OH in the early encounters and the lifetime of HONO is completely described by Eq. 3. The curvature after 30 minutes occurs because other processes, mostly the photolysis of HNO$_4$, contribute to the production of OH. However, the rates of these processes are small compared to the loss rates due to NO$_x$ and [OH] drops below background levels (see Fig. 1c).

Estimates of the oxidation of NO$_x$ and SO$_2$ by OH in the plume via reactions in (1) and (2) are shown in Figure 2. Approximately 5% of NO$_x$ and 1–2% of SO$_2$ are oxidized, mostly within the first 15 minutes. The amount of NO$_x$ oxidized by OH is largely determined by the fraction of [OH]$_0$/[NO$_x$]$_0$ in the exhaust. The fraction of SO$_2$ that is oxidized depends on the relative rates of sequences 1 and 2. For lower stratospheric daytime conditions in general, 5% of NO$_x$ and ~2% of SO$_2$ will be oxidized by OH before the plume disperses. Similar fractions are reported in modeling studies when the same [HO$_x$]$_0$/[NO$_x$]$_0$ value as determined here is used [e.g., *Danilin et al.*, 1994; *Kärcher et al.*, 1996; *Brown et al.*, 1996].

Summary and Conclusions

Based on the ratio of [HONO]$_0$/[NO$_y$]$_0$, we estimate the emission index (EI) of HO$_x$ to be 0.35 ± 0.17 gOH/kg fuel for encounter #3. Table 2 summarizes the measurements of the Concorde and ER-2 exhaust plume encounters for which accurate estimates can be made. The Concorde encounters include measurements of exhaust emitted at Mach 2 (#3) and Mach 1.7 (#4 and #5). The ER-2 emission indices represent an average of 7 plume encounters. Both the EI's of HO$_x$ and NO$_y$ are substantially smaller for the ER-2 and Mach 1.7 cases than for the Mach 2 case. This trend is consistent with the strong temperature dependence of OH and NO emission indices [*Neely and Davidson*, 1972; *McGregor et al.*, 1972].

Measurements of the number of volatile particles, thought to be composed largely of sulfuric acid, imply that at least 12–

45% of fuel sulfur is oxidized to H$_2$SO$_4$ [*Fahey et al.*, 1995a]. However, measurements of HO$_x$ suggest that only ~2% of SO$_2$ is oxidized by OH via gas-phase reactions in the plume. The discrepancy could be resolved if the particles are not primarily H$_2$SO$_4$ or if the sulfur is oxidized to SO$_3$ in the engine or in the plume by some unknown mechanism. Whether sulfur is emitted as SO$_3$, which quickly forms H$_2$SO$_4$, or as SO$_2$ determines whether sulfate aerosols form in the plume or long after the plume disperses. This formation rate directly affects the size distribution of sulfate aerosols, and will determine the impact of future HSCT emissions on aerosol surface areas throughout the stratosphere [*Weisenstein et al.*, 1996].

References

Arnold, F., et al., Measurements of Jet Aircraft Emissions, *Geophys. Res. Lett.*, *12*, 2421-2424, 1992.

Brown, R. C. et al., Aerosol dynamics in near-field aircraft plumes, *J. Geophys. Res.*, *101*, 22939-22953, 1996.

Danilin, M. Y., et al., Evolution of the concentrations of trace species in an aircraft plume: Trajectory study, *J. Geophys. Res.*, *99*, 18951-18972.

DeMore, W. B., et al., Chemical Kinetics and photochemical data for use in stratospheric modeling, evaluation number 11, *JPL Publ.* 94-26, 1994.

Fahey, D. W., et al., Emission measurements of the Concorde supersonic aircraft in the lower stratosphere, *Science*, *270*, 70-74, 1995a.

Fahey, D. W., et al., In situ observations in aircraft exhaust plumes in the lower stratosphere at midlatitudes, *J. Geophys. Res.*, *100*, 3065-3074, 1995b.

Fenter, F. F. and M. J. Rossi, Heterogeneous kinetics of HONO on H$_2$SO$_4$ solutions and on ice: activation of HCl, *J. Phys. Chem.*, *100*, 13765-13775, 1996.

Kärcher, B., M. M. Hirschberg, and P. Fabian, Small-scale chemical evolution of aircraft exhaust species at cruising altitudes, *J. Geophys. Res.*, *101*, 15169-15190, 1996.

McGregor, W. K., B. L. Seiber, and J. D. Few, Concentration of OH and NO in YJ93-GE-3 engine exhausts measured in-situ by narrow-line UV absorption, in *Proceedings of the Second Conference on CIAP*, November 1972, Cambridge, MA (A. J. Broderick, Ed.), DOT-TSC-OST-73-4, p. 214-229, (NTIS, Springfield, VA, 1973).

Neely, J. and D. L. Davidson, Emission level of the YJ93-GE-3 engine, an SST-like engine, *ibid.*, pp. 180-193.

Salawitch, R. J., et al., The distribution of hydrogen, nitrogen, and chlorine radicals in the lower stratosphere: Implications for changes in O$_3$ due to emission of NO$_y$ from supersonic aircraft, *Geophys. Res. Lett.*, *21*, 2547-2550, 1994.

Stolarski, R. S., et al., *1995 Scientific Assessment of the Atmospheric Effects of Stratospheric Aircraft*, NASA Ref. Publ. 1381, 1995.

Weisenstein, et al., Potential impact of SO$_2$ emissions from stratospheric aircraft on ozone, *Geophys. Res. Lett.*, *23*, 161-164, 1996.

Wennberg, P. O., et al., Removal of stratospheric O$_3$ by radicals: in situ measurements of OH, HO$_2$, NO, NO$_2$, ClO, and BrO, *Science*, *266*, 398-404, 1994a.

Wennberg, P. O., et. al., Aircraft-borne, laser induced fluorescence instrument for the in situ detection of hydroxyl and hydroperoxyl radicals, *Rev. Sci. Instr.*, *65*, 1858-1876, 1994b.

Williams, M. R., Emission levels of the Olympus 593 engine at the supersonic cruise conditions of the Concorde aircraft, in *Proceedings of the Second Conference on CIAP*, November 1972, Cambridge, MA (A. J. Broderick, Ed.), DOT-TSC-OST-73-4, pp. 173-179, (NTIS, Springfield, VA, 1973).

Zhang, R., M.-T. Leu, and L. F. Keyser, Heterogeneous chemistry of HONO on liquid sulfuric acid: a new mechanism of chlorine activation on stratospheric sulfate aerosols, *J. Phys. Chem.*, *100*, 339-345, 1995.

J. G. Anderson, R. C. Cohen, T. F. Hanisco, P. O. Wennberg, Department of Chemistry, Harvard University, Cambridge, MA 02138.

L. A. Del Negro, S. G. Donnelly, D. W. Fahey, R. S. Gao, E. R. Keim, K. K. Kelly, M. H. Proffitt, and R. C. Wamsley, NOAA Aeronomy Laboratory, Boulder, CO 80303.

R. J. Salawitch, Jet Propulsion Laboratory, California Institute of Technology, Pasadena, CA 91109.